Eemian Greenland ice sheet simulated with a higher-order model shows strong sensitivity to SMB forcing

Andreas Plach[1], Kerim H. Nisancioglu[1,2], Petra M. Langebroek[3], and Andreas Born[1]

[1]Department of Earth Science, University of Bergen and Bjerknes Centre for Climate Research, Bergen, Norway
[2]Centre for Earth Evolution and Dynamics, University of Oslo, Oslo, Norway
[3]NORCE Norwegian Research Centre, Bjerknes Centre for Climate Research, Bergen, Norway

Correspondence to: Andreas Plach (andreas.plach@uib.no)

Abstract. The Greenland ice sheet (GrIS) contributes increasingly to global sea level rise and its past history is a valuable reference for future sea level projections. We present ice sheet simulations for the Eemian interglacial period (~125,000 years ago), the period with the most recent warmer-than-present summer climate over Greenland. The evolution of the Eemian GrIS is simulated with a 3D higher-order ice sheet model forced with surface mass balance (SMB) derived from regional climate simulations. Sensitivity experiments with different SMB, basal friction, and ice flow approximations are discussed. We find that the SMB forcing is the controlling factor setting the Eemian minimum ice volume, emphasizing the importance of a reliable SMB model. Our results suggest that when estimating the contribution from the GrIS to sea level rise during warm periods, such as the Eemian interglacial period, the SMB forcing is more important than the representation of ice flow.

1 Introduction

The simulation of the Greenland ice sheet (GrIS) under past warmer climates is a viable way to test methods used for sea level rise projections which remain uncertain for a future warmer climate (Church et al., 2013). This study investigates ice sheet simulations for the Eemian interglacial period. The Eemian period (~125,000 years ago; thereafter 125 ka) is the most recent warmer-than-present period in Earth's history and provides an analogue for future warm climates (e.g., Yin and Berger, 2015; Clark and Huybers, 2009). The Eemian summer temperature is estimated to have been 4-5°C above present over most Arctic land areas (CAPE Last Interglacial Project Members, 2006) and ice core records from NEEM (the North Greenland Eemian Ice Drilling project in northwest Greenland, NEEM community members, 2013) indicate a local warming of 8.5±2.5°C (Landais et al., 2016) compared to pre-industrial levels. In spite of this strong warming, total gas content measurements from the Greenland ice cores at GISP2, GRIP, NGRIP, and NEEM indicate an Eemian surface elevation no more than a few hundred meters lower than present (at these locations), e.g., NEEM data indicates that the ice thickness in northwest Greenland decreased by 400±250 m between 128 and 122 ka with a surface elevation of 130±300 m lower than the present at 122 ka, resulting in a modest sea level rise estimate of 2 m (Raynaud et al., 1997; NEEM community members, 2013, c.f., Fig. 5). Nevertheless, coral reef derived global mean sea level estimates show values of at least 4 m above the present level (Overpeck et al., 2006; Kopp et al., 2013; Dutton et al., 2015). While this could suggest a reduced Antarctic ice sheet, the contribution from the GrIS to the Eemian sea level highstand remains unclear. Previous modeling studies (Letréguilly et al., 1991; Otto-Bliesner et al.,

2006; Robinson et al., 2011; Born and Nisancioglu, 2012; Stone et al., 2013; Helsen et al., 2013) used very different setup and forcing, and show highly variable results.

However, ice dynamical processes may also have contributed to the Eemian mass loss, e.g., through changes in basal conditions. Zwally et al. (2002) associate surface melt with an acceleration of GrIS flow and argue that surface melt-induced

5 enhanced basal sliding provides a mechanism for rapid, large-scale, dynamic responses of ice sheets to climate warming. Several studies have attributed the recent and future projected sea level rise from Greenland partly to dynamical responses: Price et al. (2011) use a 3D higher-order model to simulate sea level rise caused by the dynamical response of the GrIS, and they find an upper bound of 45 mm by 2100 (without assuming any changes to basal sliding in the future). This dynamical contribution is of similar magnitude as previously published SMB-induced sea level rise by 2100 (40-50 mm; Fettweis et al., 2008). Pfeffer

10 et al. (2008) provide a sea level rise estimate of 165 mm from the GrIS by 2100 based on a kinematic scenario with doubled outlet glacier velocities, i.e., doubling ice transport through topography-constrained outlet glacier gates. Furthermore, Robel and Tziperman (2016) present synthetic ice sheet simulations and argue that the early part of the deglaciation of large ice sheets is strongly influenced by an acceleration of ice streams as a response to changes in climate forcing.

In this study, we apply a computationally efficient 3D higher-order ice flow setup (alias Blatter-Pattyn; BP; Blatter, 1995;

15 Pattyn, 2003) implemented in the Ice Sheet System Model (ISSM; Cuzzone et al., 2018). Including higher-order stress gradients provides a comprehensive ice flow representation and enables us to test the importance of the ice dynamics for modeling the Eemian GrIS. Furthermore, we avoid shortcomings in regions where simpler ice flow approximations, often used in paleo applications, are inappropriate, i.e., fast flowing ice in the case of the Shallow Ice Approximation (SIA; Hutter, 1983; Greve and Blatter, 2009) and regions dominated by ice creep in the case of the Shallow Shelf Approximation (SSA; MacAyeal, 1989;

20 Greve and Blatter, 2009). The higher-order approximation is equally well suited to simulate slow as well as fast ice flow and applying it to the entire domain avoids any model-inherent discontinuities of "hybrid models" (i.e., combining SIA and SSA; Pollard and DeConto, 2009; Bueler and Brown, 2009; Pollard and DeConto, 2012; Aschwanden et al., 2016) at the boundaries between these two approximations.

Plach et al. (2018) show that the simulation of the Eemian SMB is strongly dependent on the choice of SMB model.

25 Here, we test SMB forcing derived from dynamically downscaled Eemian climate simulations and two SMB models (a full surface energy balance model and an intermediate complexity SMB model) as described in Plach et al. (2018). Furthermore, we perform sensitivity experiments varying basal friction for the entire GrIS, as well as localized changes below the outlet glaciers. With these sensitivity experiments, in combination with the 3D higher-order setup, we test the importance of the external SMB forcing and contrast this to the impact of internal ice dynamical processes for a period of climate warming.

2 Models and methods

2.1 Model description

SMB forcing

The SMB forcing used in this study is based on Eemian time slice simulations with a fast version of the Norwegian Earth
System Model (NorESM1-F; Guo et al., 2018) representing 130, 125, 120, and 115 ka conditions. These global simulations
are dynamically downscaled over Greenland with the regional climate model Modèle Atmosphérique Régional (MAR). The
SMB is calculated with (1) a full surface energy balance model implemented within MAR (MAR-SEB) and (2) an intermediate
complexity SMB model (MAR-BESSI; BErgen Snow SImulator; BESSI; Born et al., 2018). These two SMB estimates are the
best guess Eemian SMB simulations from a wider range of simulations discussed in Plach et al. (2018). MAR-SEB is used
as a control because it has been extensively validated against observations in previous studies (Fettweis, 2007; Fettweis et al.,
2013, 2017) and MAR-BESSI is used to test the sensitivity of our ice sheet simulations to the SMB forcing (c.f., discussion in
Sec. 4).

All SMB time slice simulations are calculated offline using the modern ice surface, given the lack of data constraining the
configuration of the Eemian GrIS surface. The change of the SMB with the evolving ice surface is simulated with local SMB-
altitude gradients following Helsen et al. (2012, 2013). For simplicity, the local gradients are calculated from the respective
pre-industrial SMB simulations. The SMB gradient method uses a default search radius of 150 km to derive a linear regression
of SMB versus altitude. If the lower threshold of 100 points is not reached, this search radius is extended. Since the SMB-
altitude gradients of the accumulation and the ablation zone are very different, they are calculated separately. For further
details on the SMB gradient method we refer to Helsen et al. (2012).

The transient SMB forcing from 130 to 115 ka is derived by linear interpolation of the SMBs at 130, 125, 120, and 115 ka.
The SMB during the simulation, i.e., after applying the SMB gradient method, is shown and discussed in Sec. 3. A full
description of the Eemian climate and SMB simulations is provided in Plach et al. (2018).

Ice Sheet System Model (ISSM)

ISSM is a finite-element, thermo-mechanical ice flow model which is based on conservation laws of momentum, mass, and
energy (Larour et al., 2012) — we use model version 4.13. ISSM employs an anisotropic mesh, which is typically refined by
observed surface ice velocities, allowing fast flowing ice (i.e., outlet glaciers) to be modeled at higher resolution than slow
flowing ice (i.e., interior of an ice sheet). Furthermore, ISSM offers inversion methods to ensure that an initialized model
ice sheet matches the observed (modern) ice sheet configuration (i.e., observed ice surface velocities are inverted for basal
friction or ice rheology; Morlighem et al., 2010; Larour et al., 2012). ISSM offers a range of ice flow representations —
SIA, SSA, higher-order approximations, and the full Stokes equations. For the experiments in this study, a computationally
efficient 3D higher-order configuration (Cuzzone et al., 2018) is used. This setup uses an interpolation based on higher-order
polynomials between the vertical layers, instead of the default method (a linear interpolation) which requires a much higher

number of vertical layers to capture the sharp temperature gradient at the base of an ice sheet. By using a quadratic interpolation, 5 vertical layers are sufficient to capture the thermal structure accurately, while a linear vertical interpolation requires 25 layers to achieve a similar result. This reduction in vertical layers reduces the computational demand for the thermal model, as well as for the stress balance calculations, and makes it possible to run 3D higher-order simulations thousands of years, e.g., here

5 we perform simulations over 12,000 years.

2.2 Experimental setup

All simulations run from 127 to 115 ka. We follow the Paleoclimate Modeling Intercomparison Project (PMIP4) (Otto-Bliesner et al., 2017) experimental design and initiate the Eemian simulations at 127 ka with a modern GrIS. We apply the efficient 3D higher-order ice flow setup for our experiments. To save computational time, we also use the faster 2D SSA configuration

10 of ISSM together with the same SMB forcing to efficiently identify a realistic range of the basal friction coefficients used for sensitivity experiments, i.e., we exclude basal friction coefficients which lead to unrealistic elevation changes at the deep ice core locations. Our initial (spatially varying) basal friction coefficients are derived from an inversion of observed surface velocities, i.e., an inversion algorithm chooses the basal friction coefficients in a way that the modeled velocities match the observed velocities. We use the ISSM default friction law (Larour et al., 2012; Schlegel et al., 2013) based on the empirically

15 derived friction law by Paterson (1994, p. 151):

$$\boldsymbol{\tau_{b}} = -\alpha^2 \, N_{\text{eff}} \, \boldsymbol{v_{b}} \tag{1}$$

where $\boldsymbol{\tau_b}$ is the basal shear stress (vector), α the basal friction coefficient (derived by inversion from surface velocities), N_{eff} the effective pressure of the water at the glacier base (i.e., the difference between the overburden ice stress and the water pressure), and $\boldsymbol{v_b}$ the horizontal basal velocity (vector). The effective pressure is simulated with a first order approximation

20 (Paterson, 1994):

$$N_{\text{eff}} = g \, \rho_{\text{ice}} \, H + \rho_{\text{water}} \, z_{\text{b}} \tag{2}$$

where ρ_{ice} and ρ_{water} are the densities of ice and water respectively, H the ice thickness, and z_{b} the bedrock elevation, i.e., N_{eff} evolves with H over time.

Due to the still relatively high computational demand of the 3D higher-order setup, compromises are necessary. Therefore, no

25 ice sheet spin-up is performed, and the ice sheet domain remains fixed throughout all simulations, i.e., the ice sheet is unable to grow beyond the (modern) ice domain. The basal friction coefficients (spatially varying) are held constant at the initial (modern) values. However, the basal shear stress changes with ice thickness (Eq. 1 and 2). For simplicity, the temperature prescribed at the ice surface (influencing the rheology of newly formed ice) remains fixed at pre-industrial levels as we expect negligible influence on the thermal structure over our relatively short simulation time. The SMB forcing is adjusted over time

30 using the SMB gradient method following Helsen et al. (2012). At the moment Glacial Isostatic Adjustment (GIA) is not

Table 1. ISSM model parameters

ISSM model parameters	
minimum mesh resolution (adaptive)	40 km
maximum mesh resolution (adaptive)	0.5 km
number of horizontal mesh vertices	7383
number of vertical layers	5
ice flow approximation	3D higher-order (Blatter, 1995; Pattyn, 2003)
degree of finite elements (stress balance)	P1 x P1
degree of finite elements (thermal)	P1 x P2
minimum time step (adaptive)	0.05 years
maximum time step (adaptive)	0.2 years
basal friction law	Paterson (1994, p. 151); Eq. 1 and 2
basal friction coefficient inversion cost functions	101, 103, 501
ice rheology	Cuffey and Paterson (2010, p. 75)

degree of finite elements: P1 - linear finite elements, P2 - quadratic finite elements, horizontal x vertical; inversion cost functions: 101 - absolute misfit of surface velocities, 103 - logarithmic misfit of surface velocities, 501 - absolute gradient of the basal drag coefficients

implemented in ISSM for transient simulations, i.e., the bed geometry remains fixed. Furthermore, the model setup used is incapable of modeling basal hydrology, and no ocean forcing is applied. We do not model calving, instead ice flowing out of the domain is removed.

The ice sheet is initialized with observed ice surface velocities from Rignot and Mouginot (2012) — in the updated version
5   v4Aug2014. These velocities are used to refine the anisotropic ice sheet mesh with a minimum resolution of 40 km in the slow interior to a maximum resolution of 0.5 km at the fast outlet glaciers. The ice rheology is calculated as a function of temperature following Cuffey and Paterson (2010, p. 75). Initial (modern) ice sheet surface, ice thickness, and bed topography are derived from BedMachine v3 (Morlighem et al., 2017) — in the version v2017-09-20. At the ice-bedrock interface the geothermal heat flux from Shapiro and Ritzwoller (2004) as provided in the SeaRISE dataset (Bindschadler et al., 2013) is imposed. The most
10   important parameters of the ice sheet model are summarized in Tab. 1.

Control and sensitivity experiments

The types of experiments performed are described below and summarized in Tab. 2. As discussed in Sec. 2.1, the experiments test the sensitivity to two different SMB models as well as different representations of the basal friction: The *control* experiment uses MAR-SEB SMB and unchanged (modern) basal friction; the *SMB* experiments testing the simplified, but efficient SMB
15   model, MAR-BESSI; the *basal* experiments testing spatially uniform changes to the basal friction for the entire ice sheet; the *outlets* experiments testing the sensitivity to changes of basal friction locally at the high velocity regions (>500 m/yr), i.e., the

Table 2. Overview of the performed experiments

type of experiment	SMB forcing	basal friction	ice flow approx.
control	MAR-SEB	modern	3D higher-order
SMB	MAR-BESSI	modern	3D higher-order
basal (reduced)	MAR-SEB/MAR-BESSI	0.9 * modern (entire ice sheet)	3D higher-order
basal (enhanced)	MAR-SEB/MAR-BESSI	1.1 * modern (entire ice sheet)	3D higher-order
outlets (reduced)	MAR-SEB/MAR-BESSI	0.9 (0.5) * modern (regions >500 m/yr)	3D higher-order
outlets (enhanced)	MAR-SEB/MAR-BESSI	1.1 (2.0) * modern (regions >500 m/yr)	3D higher-order
altitude	MAR-SEB/MAR-BESSI	modern	3D higher-order
relaxed	MAR-SEB	modern	3D higher-order
ice flow	MAR-SEB/MAR-BESSI	modern	2D SSA

outlet glaciers. For the whole ice sheet sensitivity tests the basal friction is multiplied by factors 0.9 and 1.1 and for the friction at the outlet glaciers alone the same factors (0.9 or 1.1) are used, but also more extreme values of 0.5 and 2.0 are applied.

In additional experiments with the more efficient SSA version of the model we explore a larger range of basal friction for the entire ice sheet (doubling/halving of basal friction similar to Helsen et al., 2013). However, we found that applying factors of

5 0.5 and 2.0 for the entire ice sheet gives unrealistic surface height changes at the deep ice core locations (not shown). Therefore, these extreme changes of basal friction are only applied to the outlet glaciers in our 3D higher-order experiments.

The *altitude* experiments test the sensitivity to the SMB-altitude feedback by neglecting this feedback. Finally, we perform *relaxed* experiments testing the sensitivity to a relaxed initial ice sheet (with the same SMB and ice dynamics as the control experiment), i.e., we start with a relaxed ice sheet which was evolved for 10 kyr under constant pre-industrial MAR-SEB SMB.

10 Since we performed most experiments first in a 2D SSA setup we compare the results of 2D SSA and 3D higher-order to show the sensitivity to *ice flow* approximation.

3 Results

The importance of the SMB forcing is illustrated in Fig. 1 showing the evolution of the Greenland ice volume in the control experiment (MAR-SEB; bold orange line) and the SMB sensitivity experiment (MAR-BESSI; bold purple line). The corre-

15 sponding sub-sets of experiments testing the basal friction are indicated in lighter colors. There is a distinct difference between the model experiments forced with the two SMBs: Forcing the ice sheet with MAR-SEB SMB (bold orange line) gives a minimum ice volume of 2.73 x 10^{15} m^3 at 124.7 ka corresponding to a sea level rise of 0.5 m — the basal sensitivity experiments give a range of 0.3 to 0.7 m (thin orange lines). On the other hand, the experiments forced with MAR-BESSI (bold purple line)
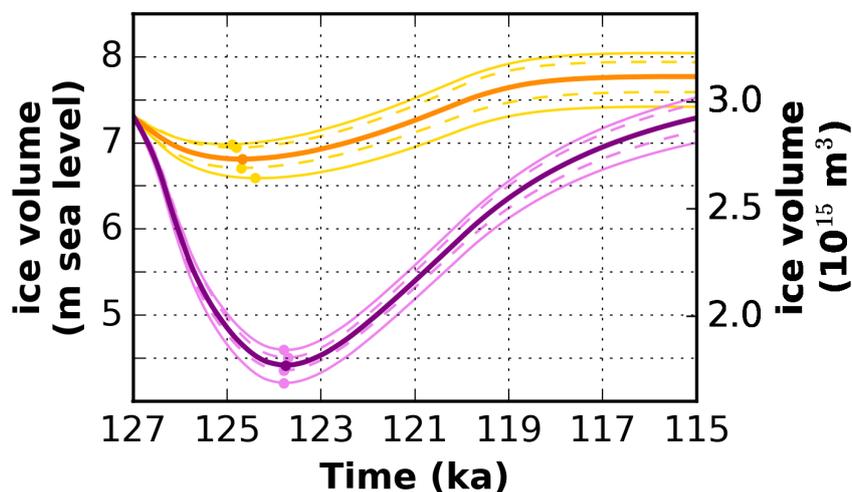
Figure 1. Evolution of the ice volume for the control experiment and the sensitivity experiments testing for SMB and basal/outlets friction. The colors indicate different SMB forcings: orange colors - MAR-SEB, purple colors - MAR-BESSI. The bold orange line is the control experiment. The bold purple is the corresponding experiment with MAR-BESSI forcing. The thin solid lines show the ±10% basal friction experiments for the entire ice sheet and the thin dashed lines show the experiments with doubling/halving of the outlets friction — lower friction experiments give lower volumes. The minimum of the respective experiments is indicated with circles. See Tab. 3 for the exact values.

give a minimum of 1.77 x 10^{15} m^3 at 123.8 ka (2.9 m sea level rise) with a range from 2.7 to 3.1 m (thin purple lines). The minimum ice volume and the corresponding sea level rise from all experiments are summarized in Tab. 3.

The basal friction sensitivity experiments with change friction for the entire ice sheet (factors 0.9 and 1.1) show the strongest influence on the ice volume compared to other basal friction experiments (thin solid lines; Fig. 1). Changing the basal fric-
5 tion locally at the outlet glaciers by factors of 0.9 and 1.1 has very little effect on the integrated ice volume (not shown), a halving/doubling of the friction at the outlet glaciers also shows a notable effect on the ice volume (0.05 to 0.15 m at the ice minimum; thin dashed lines; Fig. 1).

The importance of the SMB-altitude feedback is illustrated in Fig. 2 which shows the evolution of the ice volume with the two SMB forcings with (bold orange/purple lines) and without applying the SMB gradient method (thin orange/purple lines).
10 Neglecting the evolution of the SMB with the changing ice sheet, i.e., using the offline calculated SMBs directly, results in significantly less melt. This is particularly pronounced in the MAR-BESSI experiments, because the ablation area in this SMB forcing is larger and therefore also larger regions are affected from melt-induced surface lowering. The differences between 3D higher-order and 2D SSA are surprisingly small, particularly at the beginning of the simulations while the ice volume is decreasing (black and gray lines). The differences become larger as the ice sheet approaches a new equilibrium state towards
15 the end of the simulations. Finally, the evolution of the sensitivity experiment with a relaxed initial ice sheet (but same forcing
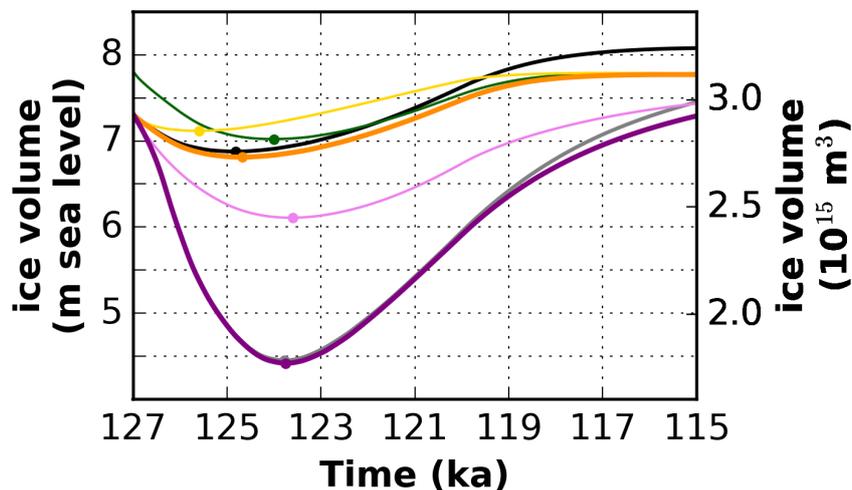
Figure 2. Evolution of the ice volume for the control experiment and the sensitivity experiments testing the influence of the SMB-altitude feedback, the relaxed initial ice sheet, and the ice flow approximation (3D higher-order vs. 2D SSA). The colors indicate different SMB forcings: orange colors - MAR-SEB, purple colors - MAR-BESSI. The bold orange line is the control experiment. The bold purple is the corresponding experiment with MAR-BESSI forcing. The light colored lines are the corresponding experiments without the SMB-altitude feedback. The dark green line is the relaxed initial ice sheet experiment with MAR-SEB forcing. 2D SSA experiments corresponding to the bold lines are shown in bold black and gray, respectively.

and ice dynamics as control experiment) is shown (darkgreen line). The volume decrease is more pronounced because the relaxed ice sheet is larger and the SMB forcing is negative enough to melt the additional ice at the margins.

Figure 3 shows the SMB forcing for the control experiment (MAR-SEB; top row) and the corresponding sensitivity experiment with MAR-BESSI (bottom row) at the beginning of simulation (127 ka), 125, 120, and 115 ka. This figure emphasizes

5 the importance of the SMB-altitude feedback, because the offline calculated SMBs (i.e., modern and initial surface) are similar between 130 and 125 ka (not shown), but the lowering of the surface in the beginning of the simulations in combination with the SMB gradient method cause the resulting SMB to become very negative in the southwest (for both MAR-SEB and MAR-BESSI) and in the northeast (particularly for MAR-BESSI). Regions with extremely low SMB at 125 ka are ice-free at the time of the simulation (ice margins are indicated with a black solid line).

10 The simulated ice sheet thickness in the control experiment (Fig. 4, top row) shows only moderate changes. However, there is significant melt in the southwest at 125 ka (actual minimum at 124.7 ka; see Fig. 7). Using the same setup, but with MAR-BESSI (Fig. 4, bottom row) gives a very different evolution of the ice thickness: The ice sheet retreat is significantly enhanced at 125 ka (actual minimum at 123.8 ka; not shown), in particular for the southwest, as well as in the northeast. The ice sheet also takes longer to recover, giving a significantly smaller ice sheet at 120 ka, partly as a consequence of the large ice loss in

15 the northeast.
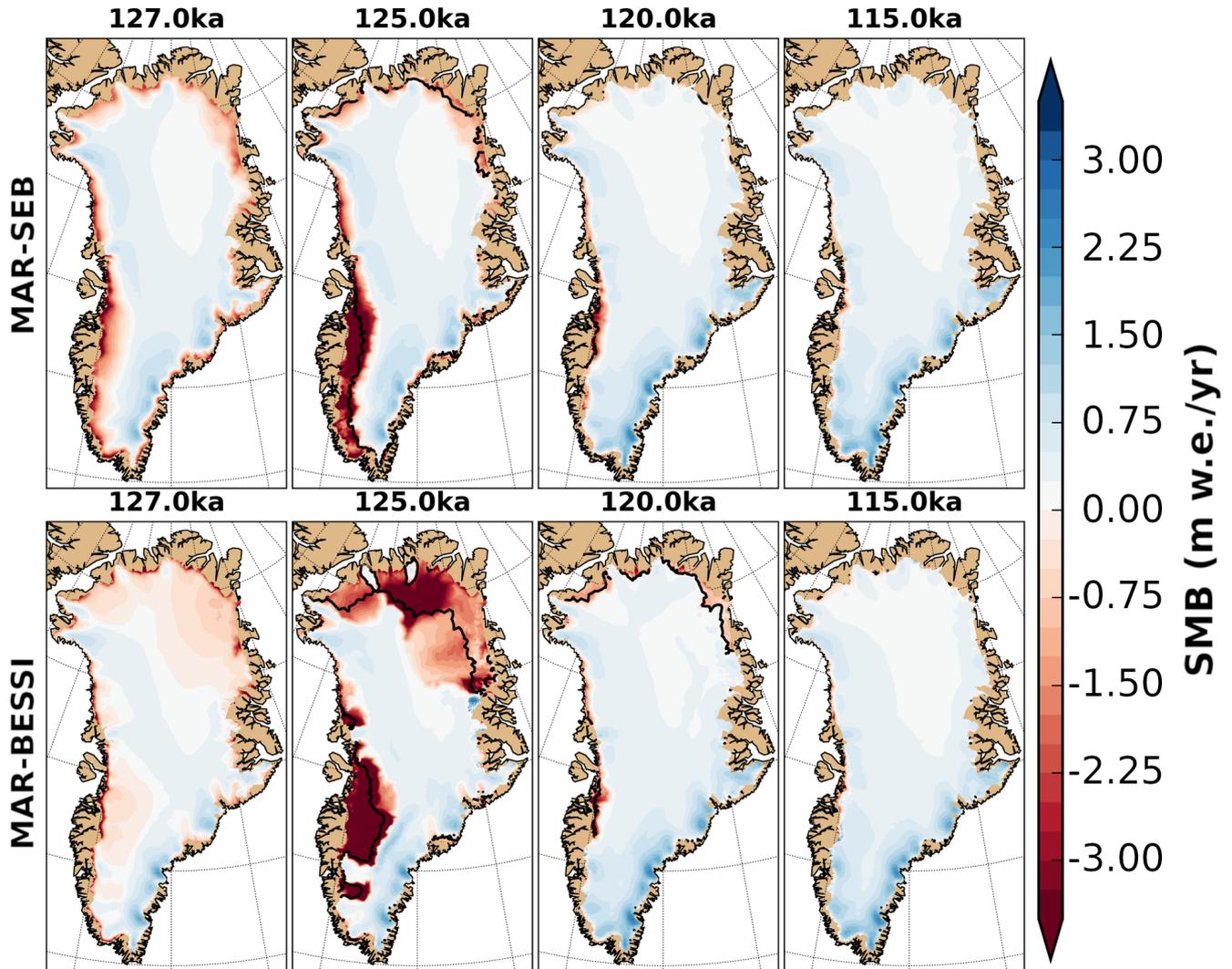
Figure 3. SMB corrected for altitude changes at 127, 125, 120, 115 ka. The ice margin is indicated with a solid black line (i.e., 10 m ice thickness). If the ice margin is not visible it is identical with the domain margin. For a consistent comparison, the ice thickness is shown at 125 ka instead of the individual minimum (124.7 ka for MAR-SEB and 123.8 ka for the MAR-BESSI).

The experiments with MAR-SEB forcing give only small changes (±200 m) in ice surface elevation at the deep ice core locations — Camp Century, NEEM, NGRIP, GRIP, Dye-3, EGRIP (Fig. 5). At most locations the surface elevation increases due to a positive SMB (which is not in equilibrium with the initial ice sheet). Only Dye-3 shows an initial lowering. Larger changes are seen in the MAR-BESSI experiments, particularly at Dye-3 and NGRIP with a maximum lowering of around 600 m, and EGRIP, where the the largest lowering is around 1500 m. In contrast to the ice volume evolution, there is a larger difference in simulated ice surface between the ice flow approximations. The 2D SSA experiments (black and grey solid lines)
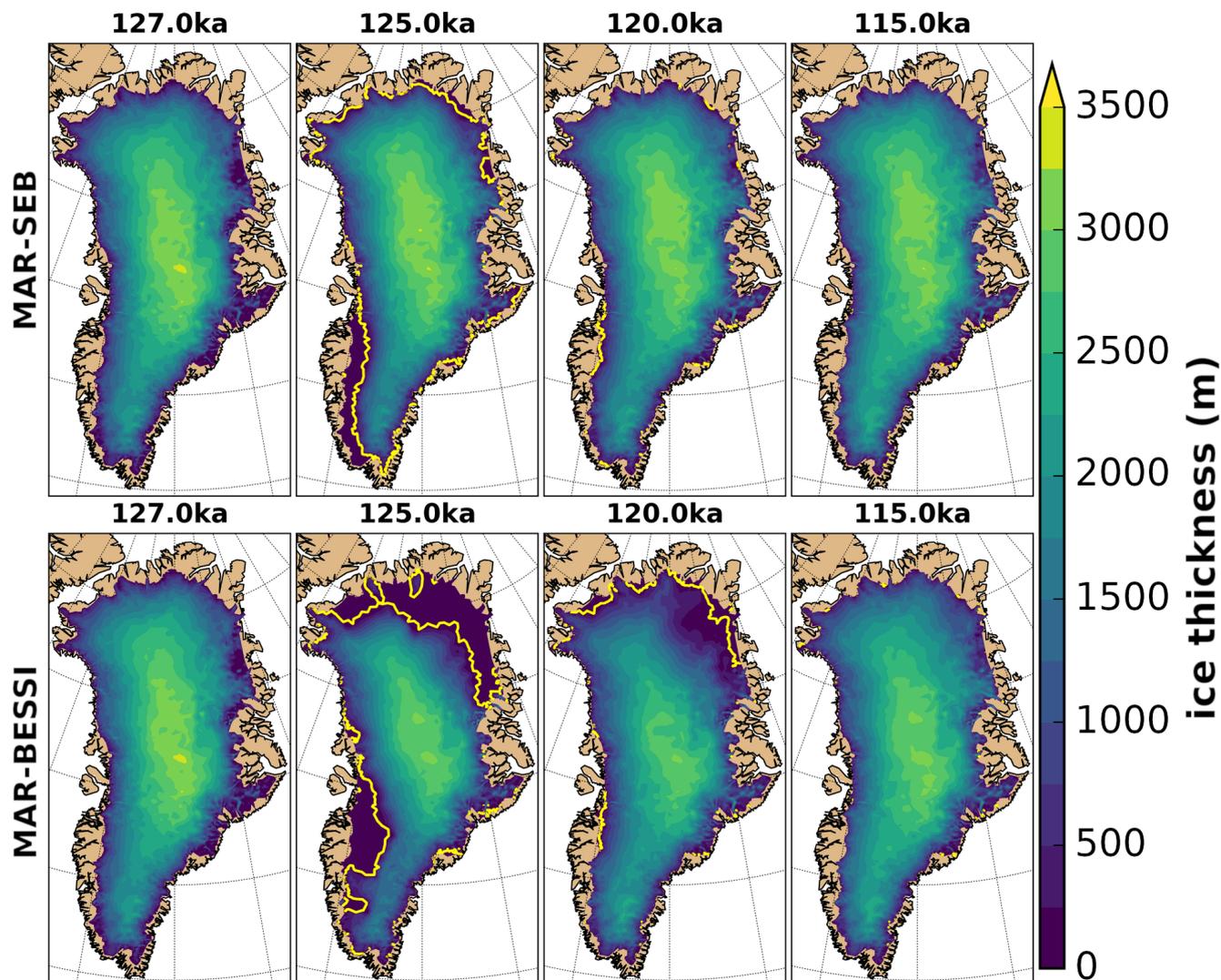
Figure 4. Ice thickness at 127, 125, 120, 115 ka. The ice margin is indicated with a solid yellow line (i.e., 10 m ice thickness). If the ice margin is not visible it is identical with the domain margin. For a consistent comparison, the ice thickness is shown at 125 ka instead of the individual minimum (124.7 ka for MAR-SEB and 123.8 ka for the MAR-BESSI).

show ice surface changes up to several hundred meters different from the 3D higher-order experiments. At Dye-3 the differences are especially pronounced. Note that for NEEM, most of the simulations lie within the reconstructed surface elevation change (gray shading).

The impact of SMB forcing, basal friction, and ice flow approximation on the ice volume minimum is shown in Fig. 6. The choice of SMB model (black bar) shows the strongest influence with ~2.5 m difference between the control experiment (with MAR-SEB) and the corresponding MAR-BESSI experiment. The SMB-altitude feedback is particularly important for MAR-
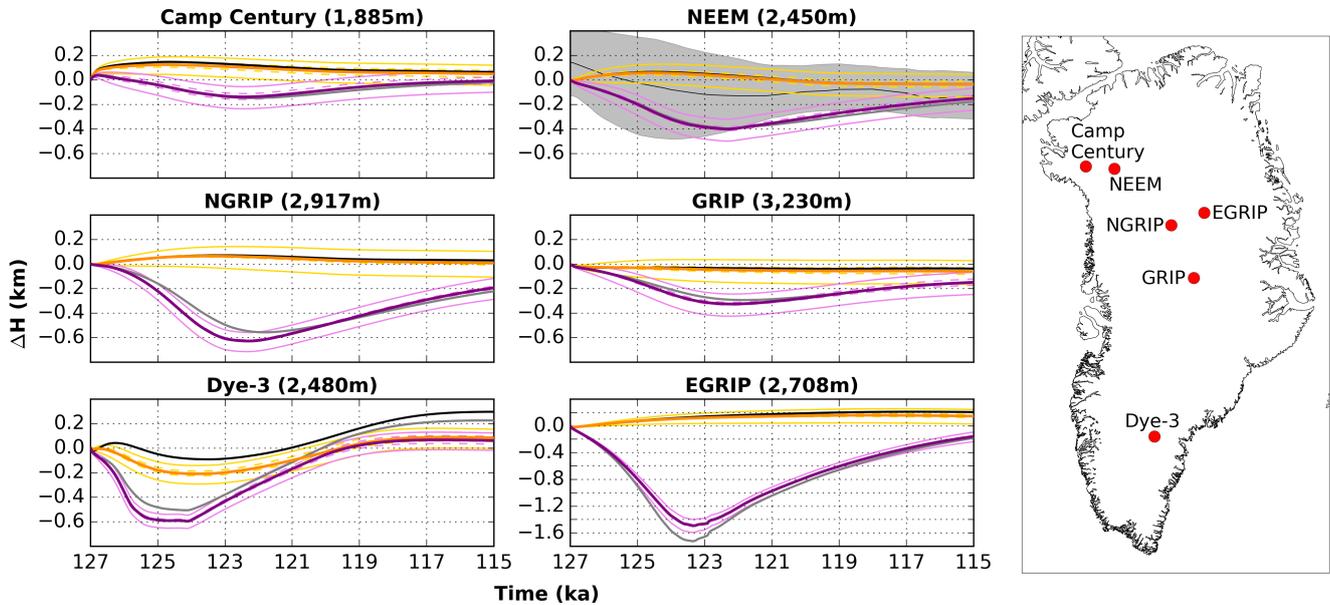
Figure 5. Ice surface evolution at Greenland ice core locations — Camp Century, NEEM, NGRIP, GRIP, and Dye-3 are shown on the same scale; EGRIP is shown on a different scale. Same color-coding as in Fig. 1, additionally including 2D SSA experiments with unchanged, modern friction in bold black and gray. Reconstruction from total gas content at NEEM are indicated with gray shading. Note that the 2D experiments are plotted in the background and therefore hardly visible in some cases, particularly at NEEM.

BESSI due to the large regions affected by melt-induced surface lowering. The sensitivity experiments with changed basal friction show a limited effect on the simulated minimum ice volume (both ice sheet as a whole and only outlets). Furthermore, using a relaxed ice sheet in the control experiments results in a ~0.3 m larger sea level rise. A comprehensive summary of the simulated ice volume minima is given in Tab. 3.

5   There are surprisingly small differences between the simulated ice thickness minimum of the control experiment (with 3D higher-order; Fig. 7; left) and the corresponding experiment using 2D SSA (Fig. 7; right). Only minor differences can be found on the east coast, where the 2D SSA experiment shows a stronger thickening than in the 3D higher-order control experiment. The complex topography in this region might explain the problem in the 2D experiment. These small differences between the ice flow approximations emphasize the controlling role of the SMB forcing and the SMB-altitude feedback.

10   However, ice flow induced thinning (e.g., due to increased basal sliding) could initiate or enhance the SMB-altitude feedback.

The impact of lower friction on the minimum ice thickness is illustrated in Fig. 8 for a selection of MAR-SEB lower friction experiments. The minimum ice thickness for the control experiment is shown on the left. Lowering the friction at the base of the entire ice sheet by a factor of 0.9 (Fig. 8; middle) results in a thinning on the order of 100 m in large parts of the ice sheet. Interestingly, in the northeast this effect is inverted, i.e., a Greenland-wide lowering of friction leads to a thickening in the

15   northeast margin. This is because a large amount of ice drains towards this region: a faster inflow leads to a build up of ice at the outlet. A closer look at the margins reveals that this observed build up of ice is visible at most outlets, including Jakobshavn

Table 3. Summary of the simulated ice sheet minima for all experiments

experimental setup	SLR [m] rel. to initial	ΔSLR [m] at resp. minima	Minimum GrIS volume ($10^{15} m^3$)
control MAR-SEB	**0.51**	**0.00**	**2.73**
_basal_*0.9 MAR-SEB	0.73	+0.22	2.64
_basal_*1.1 MAR-SEB	0.33	-0.17	2.80
_outlets_*0.9 (*0.5) MAR-SEB	0.53 (0.61)	+0.02 (+0.10)	2.72 (2.69)
_outlets_*1.1 (*2.0) MAR-SEB	0.48 (0.36)	-0.02 (-0.15)	2.74 (2.79)
altitude MAR-SEB	0.18	-0.32	2.86
relaxed MAR-SEB	0.79	+0.28	2.82
ice flow (2D) MAR-SEB	0.43	-0.07	2.76
SMB MAR-BESSI	2.90	0.00	1.77
_basal_*0.9 MAR-BESSI	3.10	+0.20	1.69
_basal_*1.1 MAR-BESSI	2.72	-0.18	1.84
_outlets_*0.9 (*0.5) MAR-BESSI	2.90 (2.95)	+0.00 (+0.05)	1.77 (1.75)
_outlets_*1.1 (*2.0) MAR-BESSI	2.87 (2.80)	-0.03 (-0.10)	1.78 (1.81)
altitude MAR-BESSI	1.20	-1.70	2.45
ice flow (2D) MAR-BESSI	2.85	-0.05	1.79

For the outlet glacier sensitivity experiments, the basal friction in regions with > 500 m/yr is changed.
Sea level rise (SLR) values are relative to the initial ice sheet at 127 ka, i.e., the modern ice sheet for all
experiments except the relaxed initial ice sheet experiment. The lost ice volume is equally spread over
the modern ocean area. ΔSLR refers to anomalies relative to the respective SMB forcing experiments
with unchanged friction.

Isbræ in the southwest, but less pronounced. Lowering the basal friction only at the outlet glaciers by a factor of 0.5 (Fig. 8; right) leads to a local thinning around the outlet glaciers of several hundred meters. Note that the thinning affects ice thickness upstream from the outlet region.

The ice velocities in the basal sensitivity experiments indicate that a Greenland-wide reduction of basal friction by a factor of 0.9 leads to a speed up of the outlet glaciers by up to several 100 m/year (Fig. 9; middle). Reducing the friction at the outlet glaciers by a factor of 0.5 has a large, but local effect on the ice velocity (Fig. 9; right). Both, this local speed-up as well as the local thinning in the 0.5 * lower outlet friction experiment (Fig. 8; right) show that the outlet friction have a limited effect on regions further upstream.
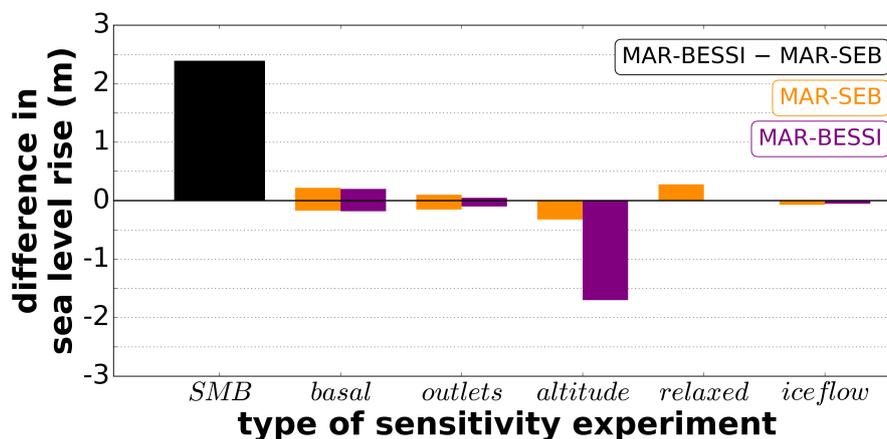
Figure 6. Differences in sea level estimates given by the sensitivity experiments. *SMB* (black) refers to the difference between the two SMB forcings (incl. the SMB-altitude feedback). *basal/outlets* refers to sensitivity experiments with changes friction for the entire ice sheet/outlets. *altitude* shows the experiments without the SMB-altitude feedback. *relaxed* uses a relaxed, initial ice sheet, and *ice flow* shows the difference between 3D higher-order and 2D SSA approximation. The results of the sensitivity experiments are shown in orange (MAR-SEB) and purple (MAR-BESSI). The exact values are given in Tab. 3.

4 Discussion

Changing the SMB forcing — between a full surface energy balance model (MAR-SEB) and an intermediate complexity SMB model (MAR-BESSI) — gives the biggest difference in the simulated Eemian ice sheet evolution (Fig. 6). MAR-SEB and MAR-BESSI are two Eemian SMBs from a wide range of simulations analyzed in Plach et al. (2018). Note that the same global climate model (NorESM) is used as a boundary condition for the SMB models. All available NorESM global climate simulations covering the Eemian period are downscaled over Greenland using the regional climate model MAR. Here we neglect the uncertainties relating to the global climate forcing. Including such uncertainties is beyond the scope of this study. Instead the reader is referred to the discussion in Plach et al. (2018).

Our control experiment with the 3D higher-order ice flow, modern, unchanged basal friction, and forced with MAR-SEB shows little melting (0.5 m sea level rise), while MAR-BESSI causes a large ice sheet reduction (2.9 m sea level rise). The basal sensitivity experiments give a range of approx. ±0.2 m for both SMB models, where the Greenland-wide friction change shows the largest influence on the minimum ice volume. Decreasing/increasing friction at the outlet glaciers by a factor of 0.9/1.1 shows mainly local thinning/thickening at the outlets (Fig. 8) with limited effects on the total ice volume (Fig. 1). However, doubling/halving friction at the outlet glaciers leads to an ice volume change equivalent to 0.05-0.15 m sea level.

The importance of coupling the climate (SMB) and the ice sheet has been demonstrated in previous studies, e.g., recently for regional climate models in a projected future climate assessment by Le clec'h et al. (2017). However, running a high resolution regional climate model over several thousand years is not possible at present due to the exceedingly high computational cost.
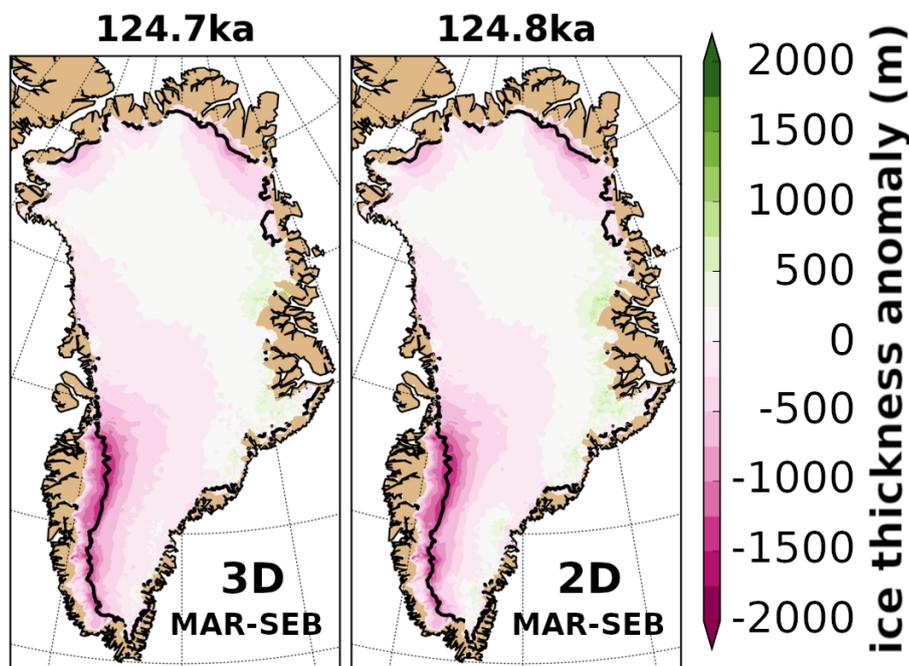
Figure 7. Ice thickness anomalies simulated with the control 3D higher-order (left) and ice flow 2D SSA (right) at the respective Eemian ice minimum. Relative to the initial 127 ka ice sheet (i.e., modern ice sheet). The respective minimum time of the individual experiments is indicated on the top. The ice margin is indicated with a black bold line (i.e., 10 m ice thickness). If the ice margin is not visible it is identical with the domain margin.

This is even more true when the goal is to run an ensemble of long sensitivity simulations as presented here. Although a coupling between the ice sheet and climate model is absent in our simulations, we do account for the SMB-altitude feedback by applying the SMB gradient method. The SMB becomes significantly lower as the ice surface is lowered: neglecting the SMB-altitude feedback gives less than half the volume reduction (MAR-SEB: 0.2 vs. 0.5 m; MAR-BESSI: 1.2 vs. 2.9 m; Fig. 2 and 6).

    Towards the end of the simulations, all model experiments develop a new equilibrium ice sheet which is larger than the initial state (Fig. 1 and 2). This relaxation towards a larger ice sheet is likely due to the initial pre-industrial ice sheet configuration not being in equilibrium with the initial SMB forcing. A 10 kyr simulation with constant pre-industrial SMB gives an ~10 % larger "relaxed" modern ice sheet which is in equilibrium with the forcing. Sensitivity experiments with this "relaxed" initial ice sheet (~0.5 m larger initial state) result in a ~0.3 m larger sea level rise (at the minimum) compared to the control experiment. We don't expect the 127 ka GrIS to be in equilibrium with pre-industrial forcing. However, the "relaxed" experiment demonstrates the impact of a larger initial ice sheet on our estimates of the contribution of Greenland to the Eemian sea level high-stand.

    Furthermore, the simplified initialization implies that the thermal structure of the simulated ice sheet is lacking the history of a full glacial-interglacial cycle, i.e., the ice rheology of our ice sheet is different to an ice sheet which is spun-up through a
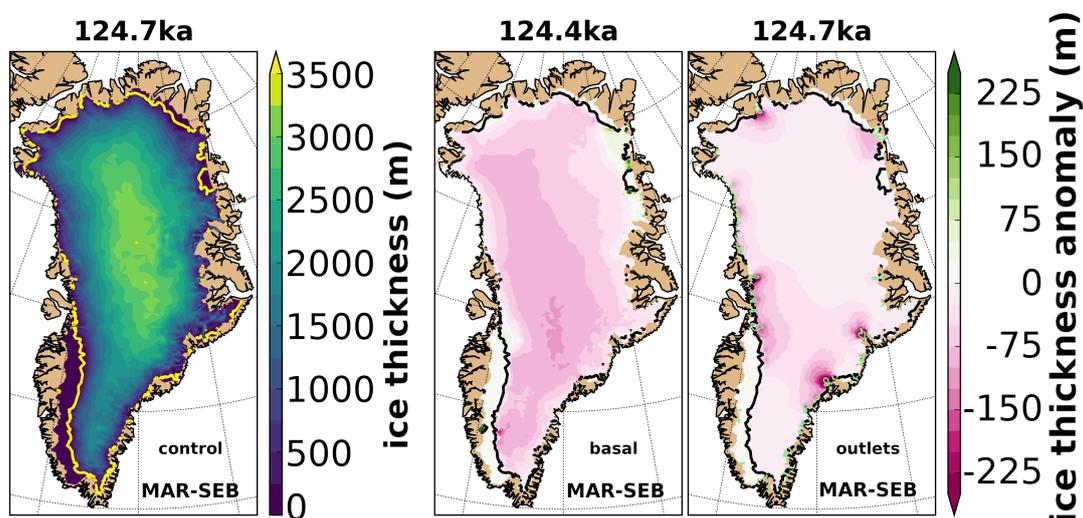
Figure 8. Minimum ice thickness of the control experiment (left) and the basal*0.9/outlets*0.5 reduced friction experiments (middle/right) at the time of the respective ice minimum (time indicated on top). basal*0.9 and outlets*0.5 are shown as anomaly relative to the control experiment. The ice margin is indicated with a yellow/black bold line (10 m ice thickness). If the ice margin is not visible it is identical with the domain margin. The outlet regions are indicated with bright green contours.
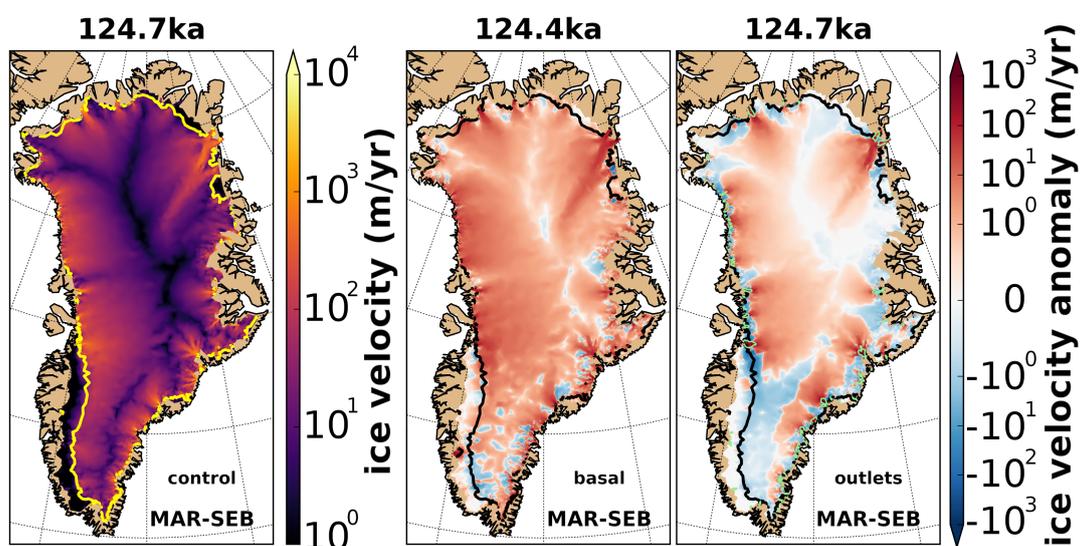
Figure 9. Ice velocity of the minimum ice sheet in the control experiment (left) and the basal*0.9/outlets*0.5 reduced friction experiments (middle/right) at the time of the respective ice minimum (time indicated on top). basal*0.9 and outlets*0.5 are shown as anomaly relative to the control experiment. The ice margin is indicated with a yellow/black bold line (i.e., 10 m ice thickness). If the ice margin is not visible it is identical with the domain margin. The outlet regions are indicated with bright green contours.

glacial cycle. Helsen et al. (2013) demonstrate the importance of the ice rheology for the pre-Eemian ice sheet size. They find differences of up to 20% in initial ice volume after a spin-up forced with different glacial temperatures. A viable way to test the influence of the thermal structure on the ice rheology would be to perform additional sensitivity experiments. However, such rheology experiments can only be performed in the 3D higher-order setup (the 2D SSA setup neglects vertical shear) and the

5   computational resources to run additional 3D experiments are limited.

The results of the 3D higher-order and 2D SSA experiments are similar, in particular for the simulated minimum ice volume. However, the difference in ice volume becomes larger towards the end of the simulations under less negative SMB forcing. Furthermore, the ice surface evolution at the deep ice core locations differs substantially for the two ice flow approximations.

The strong similarities between 3D higher-order and 2D SSA — also noted by Larour et al. (2012) using ISSM for centennial

10   simulations — are likely related to the inversion of the friction coefficients from observed velocities. The dynamical deficiencies of the 2D SSA ice flow are partly compensated by the inversion algorithm: this algorithm chooses basal conditions such that the model simulates surface velocities as close to the observations as possible. The relatively small difference between the 3D higher-order and 2D SSA experiments indicates that the SMB forcing is more important in our simulations than the ice dynamics.

15   Basal hydrology is neglected in our simulations because it is not well understood and therefore difficult to implement in a robust way. Furthermore, an implementation of basal hydrology would increase the computational demand of our simulations and make them unfeasible on the millennial time scales we are investigating. We recognize that basal hydrology might have been important for the recent observed acceleration of Greenland outlet glaciers (e.g., Aschwanden et al., 2016). Therefore, the impact of changing basal hydrology at the outlet glaciers is tested by varying the friction at the bed of the outlet glaciers.

20   Although we are not simulating basal hydrology explicitly, we can assess its possible consequences — a slow down or speed up of the outlet glaciers.

Furthermore, we neglect ocean forcing and processes including grounding line migration due to their complexity and because the minimum Eemian ice sheet is likely to have been land based. Note, however, that these processes are thought to be important for the recent observed changes at Greenland's outlet glaciers (Straneo and Heimbach, 2013). Tabone et al. (2018) investigate

25   the influence of ocean forcing on the Eemian GrIS. Their sensitivity experiments indicate that the Eemian minimum is governed by the atmospheric forcing, due to the lack of contact between the ice margin and the ocean. However, their estimated relative Eemian sea level rise is dependent on the ocean forcing, as it influences their pre-Eemian ice sheet size.

Our simulations, starting with the orbital configuration and greenhouse gas levels at 127 ka, are initiated with the observed modern geometry of the Greenland ice sheet (following the PMIP4 protocol; Otto-Bliesner et al., 2017). One advantage of

30   this procedure, is that is allows for a basal friction configuration based on inverted observed modern surface velocities. A spin-up over a glacial cycle, without adapting basal friction, would be unrealistic. Furthermore, a spin-up would require ice sheet boundary migration, i.e., implementation of calving, grounding line migration, and a larger ice domain. This would be challenging as the resolution of the ISSM mesh is based on observed surface velocities. Furthermore, a time adaptive mesh, to allow for the migration of the high resolution mesh with the evolving ice streams, would be adventurous but challenging

35   to implement. Furthermore, the lack of a robust estimate of the pre-Eemian GrIS size and the uncertainties in climate over
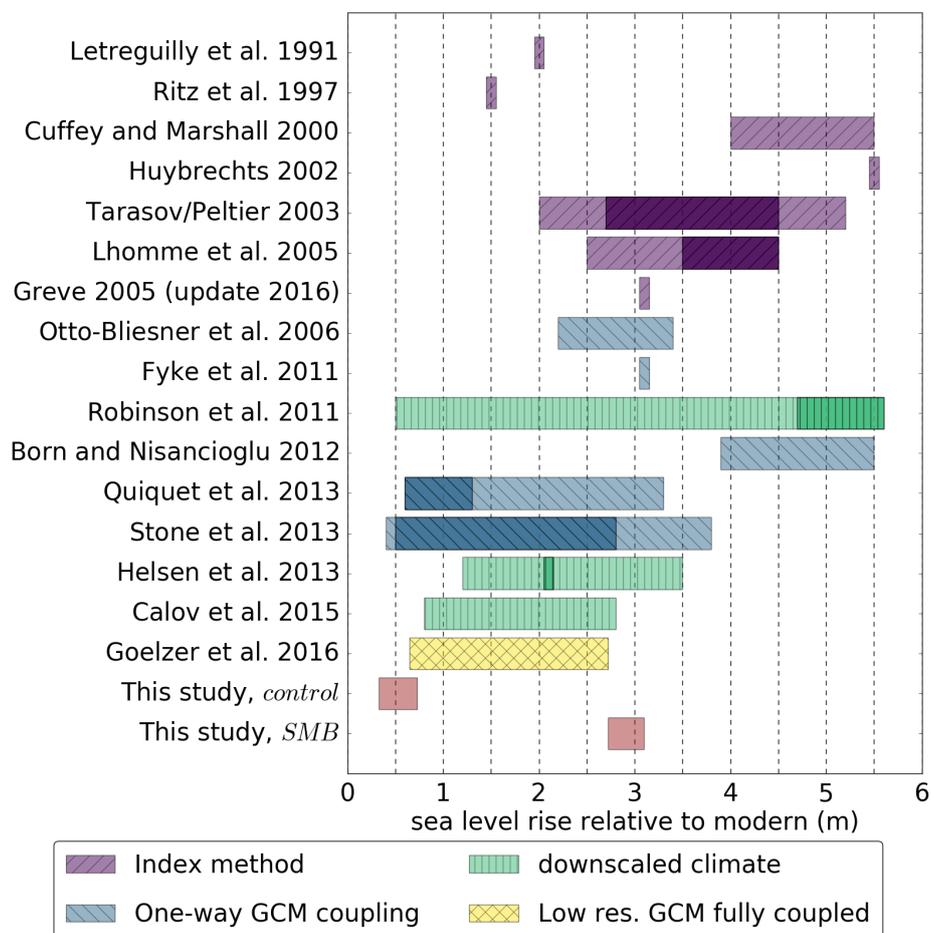
Figure 10. Simulated sea level rise contributions from this study and previous Eemian studies. For this study the results of the *control* (MAR-SEB; lower bound) and the *SMB* experiments (MAR-BESSI; upper bound) are shown (the ranges show the results of the respective basal/outlets fraction sensitivity experiments). Previous studies are color-coded according to the type of climate forcing used. More likely estimates are indicated with darker colors if provided in the respective studies. A common sea level rise conversion (distributing the meltwater volume equally on Earth's ocean area) is applied to Greve (2005), Robinson et al. (2011), Born and Nisancioglu (2012), Quiquet et al. (2013), Helsen et al. (2013), and Calov et al. (2015).

the last glacial cycle would introduce even more uncertainties to the initial ice sheet, which is outside the scope of this study. However, in the future, once these hurdles have been overcome, a 3D higher-order spin-up covering the last glacial cycle will be attempted.

Our simulated impact of the GrIS on the Eemian global mean sea level high-stand in our control experiment (~0.5 m) is low compared to previous Eemian model studies (Fig. 10). While, the sensitivity experiments with the second, less advanced, SMB model (MAR-BESSI) show a significantly larger contribution to sea level (~3.0 m), closer to previous estimates. Both SMB

models are forced with a regionally downscaled climate based on experiments with the global climate model NorESM. This emphasises the importance of both an accurate global climate simulation and a realistic SMB model in estimating the GrIS minimum in a warm climate such as the Eemian interglacial period.

5 Conclusions

5   This study emphasizes the importance of accurate surface mass balance (SMB) forcing over detailed ice sheet physics when simulating the past evolution of the Eemian Greenland ice sheet. Our experiments with two SMBs — a full surface energy balance model and an intermediate complexity SMB model — result in different Eemian sea level contributions (~0.5 to 3.0 m) when forced with the same detailed regional climate over Greenland. Furthermore, we show the importance of the SMB-altitude feedback; neglecting this feedback reduces the simulated sea level contribution by more than 50%. Moreover, our simulations

10   indicate a limited influence of the ice flow approximation on the simulated minimum ice volume. For simulations of the long-term response of the Greenland ice sheet to warmer climates, such as the Eemian interglacial period, efforts should focus on improving the representation of the SMB rather than the ice flow.

6 Code availability

The ISSM code can be freely downloaded from http://issm.jpl.nasa.gov (last accessed: 18.10.2018). Model scripts and other

15   datasets can be obtained upon request from the corresponding author. The NorESM model code can be obtained upon request. Instructions on how to obtain a copy are given at: https://wiki.met.no/noresm/gitbestpractice (last accessed: 18.10.2018). BESSI is under active development. For more information contact Andreas Born (andreas.born@uib.no). The MAR code is available at: http://mar.cnrs.fr (last accessed: 18.10.2018).

7 Data availability

20   The ISSM simulations and the MAR-SEB and MAR-BESSI SMBs are available upon request from the corresponding author. The SeaRISE dataset used is freely available at: http://websrv.cs.umt.edu/isis/images/e/e9/Greenland_5km_dev1.2.nc. (last accessed: 18.10.2018)

Author contributions. AP and KHN designed the study with contributions from PML and AB. AP performed the ISSM simulations, made the figures and wrote the text with input from KHN, PML, AB.

25   *Competing interests.* The authors declare that they have no conflict of interest.

Acknowledgements. The research leading to these results has received funding from the European Research Council under the European
Community's Seventh Framework Programme (FP7/2007-2013) / ERC grant agreement 610055 as part of the ice2ice project. The simulations
were performed on resources provided by UNINETT Sigma2; the National Infrastructure for High Performance Computing and Data Storage
in Norway (NN4659k; NS4659k). PML was supported by the RISES project of the Centre for Climate Dynamics at the Bjerknes Centre for
5   Climate Research. We thank J.K. Cuzzone for assisting in setting up the higher-order ISSM runs and M.M. Helsen for helping with the SMB
gradient method. Furthermore, we thank B. de Fleurian for helping to resolve technical issues with ISSM.

References

Aschwanden, A., Fahnestock, M. A., and Truffer, M.: Complex Greenland outlet glacier flow captured, Nature Communications, 7, 10 524, https://doi.org/10.1038/ncomms10524, 2016.

Bindschadler, R. A., Nowicki, S., Abe-Ouchi, A., Aschwanden, A., Choi, H., Fastook, J., Granzow, G., Greve, R., Gutowski, G., Herzfeld,
5   U., Jackson, C., Johnson, J., Khroulev, C., Levermann, A., Lipscomb, W. H., Martin, M. A., Morlighem, M., Parizek, B. R., Pollard,
     D., Price, S. F., Ren, D., Saito, F., Sato, T., Seddik, H., Seroussi, H., Takahashi, K., Walker, R., and Wang, W. L.: Ice-sheet model
     sensitivities to environmental forcing and their use in projecting future sea level (the SeaRISE project), Journal of Glaciology, 59, 195–
     224, https://doi.org/10.3189/2013JoG12J125, 2013.

Blatter, H.: Velocity and stress fields in grounded glaciers: a simple algorithm for including deviatoric stress gradients, Journal of Glaciology,
10   41, 333–344, https://doi.org/10.3189/S002214300001621X, 1995.

Born, A. and Nisancioglu, K. H.: Melting of Northern Greenland during the last interglaciation, The Cryosphere, 6, 1239–1250, https://doi.org/10.5194/tc-6-1239-2012, 2012.

Born, A., Imhof, M., and Stocker, T. F.: A surface energy and mass balance model for simulations over multiple glacial cycles, submitted to The Cryosphere Discuss., 2018.

15   Bueler, E. and Brown, J.: Shallow shelf approximation as a "sliding law" in a thermomechanically coupled ice sheet model, Journal of Geophysical Research: Earth Surface, 114, F03 008, https://doi.org/10.1029/2008JF001179, 2009.

Calov, R., Robinson, A., Perrette, M., and Ganopolski, A.: Simulating the Greenland ice sheet under present-day and palaeo constraints including a new discharge parameterization, The Cryosphere, 9, 179–196, https://doi.org/10.5194/tc-9-179-2015, 2015.

CAPE Last Interglacial Project Members: Last Interglacial Arctic warmth confirms polar amplification of climate change, Quaternary Science
20   Reviews, 25, 1383–1400, https://doi.org/10.1016/j.quascirev.2006.01.033, 2006.

Church, J., Clark, P. U., Cazenave, A., Gregory, J. M., Jevrejeva, S., Levermann, A., Merrifield, M., Milne, G., Nerem, R., Nunn, P., Payne,
     A. J., Pfeffer, W., Stammer, D., and Unnikrishnan, A.: Sea Level Change, in: Climate Change 2013: The Physical Science Basis. Contribu-
     tion of Working Group I to the Fifth Assessment Report of the Intergovernmental Panel on Climate Change [Stocker, T.F., D. Qin, G.-K.
     Plattner, M. Tignor, S.K. Allen, J. Boschung, A. Nauels, Y. Xia, V. Bex and P.M. Midgley (eds.)], pp. 1137–1216, Cambridge University
25   Press, Cambridge, United Kingdom and New York, NY, USA, 2013.

Clark, P. U. and Huybers, P.: Interglacial and future sea level: Global change, Nature, 462, 856–857, http://doi.org/10.1038/462856a, 2009.

Cuffey, K. M. and Paterson, W.: The Physics of Glaciers, Elsevier Science, Burlington, 4th edn., 2010.

Cuzzone, J. K., Morlighem, M., Larour, E., Schlegel, N., and Seroussi, H.: Implementation of higher-order vertical finite elements in ISSM
     v4.13 for improved ice sheet flow modeling over paleoclimate timescales, Geosci. Model Dev., 11, 1683–1694, https://doi.org/10.5194/
30   gmd-11-1683-2018, 2018.

Dutton, A., Carlson, A. E., Long, A. J., Milne, G. A., Clark, P. U., DeConto, R., Horton, B. P., Rahmstorf, S., and Raymo, M. E.: Sea-level
     rise due to polar ice-sheet mass loss during past warm periods, Science, 349, aaa4019, https://doi.org/10.1126/science.aaa4019, 2015.

Fettweis, X.: Reconstruction of the 1979–2006 Greenland ice sheet surface mass balance using the regional climate model MAR, The
     Cryosphere, 1, 21–40, https://doi.org/10.5194/tc-1-21-2007, 2007.

35   Fettweis, X., Hanna, E., Gallée, H., Huybrechts, P., and Erpicum, M.: Estimation of the Greenland ice sheet surface mass balance for the
     20th and 21st centuries, The Cryosphere, 2, 117–129, https://doi.org/10.5194/tc-2-117-2008, 2008.

Fettweis, X., Franco, B., Tedesco, M., Angelen, J. H. v., Lenaerts, J. T. M., Broeke, M. R. v. d., and Gallée, H.: Estimating the Greenland ice
sheet surface mass balance contribution to future sea level rise using the regional atmospheric climate model MAR, The Cryosphere, 7,
469–489, https://doi.org/10.5194/tc-7-469-2013, 2013.

Fettweis, X., Box, J. E., Agosta, C., Amory, C., Kittel, C., Lang, C., van As, D., Machguth, H., and Gallée, H.: Reconstructions of the
1900–2015 Greenland ice sheet surface mass balance using the regional climate MAR model, The Cryosphere, 11, 1015–1033, https:
//doi.org/10.5194/tc-11-1015-2017, 2017.

Greve, R.: Relation of measured basal temperatures and the spatial distribution of the geothermal heat flux for the Greenland ice sheet,
Annals of Glaciology, 42, 424–432, https://doi.org/10.3189/172756405781812510, 2005.

Greve, R. and Blatter, H.: Dynamics of ice sheets and glaciers, Springer, Berlin Heidelberg, https://doi.org/10.1007/978-3-642-03415-2,
2009.

Guo, C., Bentsen, M., Bethke, I., Ilicak, M., Tjiputra, J., Toniazzo, T., Schwinger, J., and Otterå, O. H.: Description and evaluation of
NorESM1-F: A fast version of the Norwegian Earth System Model (NorESM), Geoscientific Model Development Discussions, pp. 1–37,
https://doi.org/10.5194/gmd-2018-217, 2018.

Helsen, M. M., Wal, R. S. W. v. d., Broeke, M. R. v. d., Berg, W. J. v. d., and Oerlemans, J.: Coupling of climate models and ice sheet
models by surface mass balance gradients: application to the Greenland Ice Sheet, The Cryosphere, 6, 255–272, https://doi.org/10.5194/
tc-6-255-2012, 2012.

Helsen, M. M., Berg, W. J. v. d., Wal, R. S. W. v. d., Broeke, M. R. v. d., and Oerlemans, J.: Coupled regional climate–ice-sheet simulation
shows limited Greenland ice loss during the Eemian, Clim. Past, 9, 1773–1788, https://doi.org/10.5194/cp-9-1773-2013, 2013.

Hutter, K.: Theoretical Glaciology: Material Science of Ice and the Mechanics of Glaciers and Ice Sheets, D. Reidel Publishing Company,
Dordrecht, The Netherlands, 1983.

Kopp, R. E., Simons, F. J., Mitrovica, J. X., Maloof, A. C., and Oppenheimer, M.: A probabilistic assessment of sea level variations within
the last interglacial stage, Geophysical Journal International, p. ggt029, https://doi.org/10.1093/gji/ggt029, 2013.

Landais, A., Masson-Delmotte, V., Capron, E., Langebroek, P. M., Bakker, P., Stone, E. J., Merz, N., Raible, C. C., Fischer, H., Orsi, A.,
Prié, F., Vinther, B., and Dahl-Jensen, D.: How warm was Greenland during the last interglacial period?, Clim. Past, 12, 1933–1948,
https://doi.org/10.5194/cp-12-1933-2016, 2016.

Larour, E., Seroussi, H., Morlighem, M., and Rignot, E.: Continental scale, high order, high spatial resolution, ice sheet modeling using the
Ice Sheet System Model (ISSM), Journal of Geophysical Research: Earth Surface, 117, F01 022, https://doi.org/10.1029/2011JF002140,
2012.

Le clec'h, S., Fettweis, X., Quiquet, A., Dumas, C., Kageyama, M., Charbit, S., Wyard, C., and Ritz, C.: Assessment of the Greenland ice
sheet – atmosphere feedbacks for the next century with a regional atmospheric model fully coupled to an ice sheet model, The Cryosphere
Discuss., 2017, 1–31, doi:10.5194/tc-2017-230, https://www.the-cryosphere-discuss.net/tc-2017-230/, 2017.

Letréguilly, A., Reeh, N., and Huybrechts, P.: The Greenland ice sheet through the last glacial-interglacial cycle, Palaeogeogr., Palaeoclima-
tol., Palaeoecol. (Global Planet. Change Sect.), 90, 385–394, https://doi.org/10.1016/S0031-0182(12)80037-X, 1991.

MacAyeal, D. R.: Large-scale ice flow over a viscous basal sediment: Theory and application to ice stream B, Antarctica, Journal of Geo-
physical Research: Solid Earth, 94, 4071–4087, https://doi.org/10.1029/JB094iB04p04071, 1989.

Morlighem, M., Rignot, E., Seroussi, H., Larour, E., Ben Dhia, H., and Aubry, D.: Spatial patterns of basal drag inferred using control
methods from a full-Stokes and simpler models for Pine Island Glacier, West Antarctica, Geophysical Research Letters, 37, L14 502,
https://doi.org/10.1029/2010GL043853, 2010.

Morlighem, M., Williams, C. N., Rignot, E., An, L., Arndt, J. E., Bamber, J. L., Catania, G., Chauché, N., Dowdeswell, J. A., Dorschel, B., Fenty, I., Hogan, K., Howat, I., Hubbard, A., Jakobsson, M., Jordan, T. M., Kjeldsen, K. K., Millan, R., Mayer, L., Mouginot, J., Noël, B. P. Y., O'Cofaigh, C., Palmer, S., Rysgaard, S., Seroussi, H., Siegert, M. J., Slabon, P., Straneo, F., van den Broeke, M. R., Weinrebe, W., Wood, M., and Zinglersen, K. B.: BedMachine v3: Complete Bed Topography and Ocean Bathymetry Mapping of Greenland From
5   Multibeam Echo Sounding Combined With Mass Conservation: BEDMACHINE GREENLAND V3, Geophysical Research Letters, 44, 11,051–11,061, https://doi.org/10.1002/2017GL074954, 2017.

NEEM community members: Eemian interglacial reconstructed from a Greenland folded ice core, Nature, 493, 489–494, https://doi.org/10.1038/nature11789, 2013.

Otto-Bliesner, B. L., Marshall, S. J., Overpeck, J. T., Miller, G. H., and Hu, A.: Simulating Arctic climate warmth and icefield retreat in the
10   last interglaciation, science, 311, 1751–1753, https://doi.org/10.1126/science.1120808, 2006.

Otto-Bliesner, B. L., Braconnot, P., Harrison, S. P., Lunt, D. J., Abe-Ouchi, A., Albani, S., Bartlein, P. J., Capron, E., Carlson, A. E., Dutton, A., Fischer, H., Goelzer, H., Govin, A., Haywood, A., Joos, F., LeGrande, A. N., Lipscomb, W. H., Lohmann, G., Mahowald, N., Nehrbass-Ahles, C., Pausata, F. S. R., Peterschmitt, J.-Y., Phipps, S. J., Renssen, H., and Zhang, Q.: The PMIP4 contribution to CMIP6 – Part 2: Two interglacials, scientific objective and experimental design for Holocene and Last Interglacial simulations, Geosci. Model Dev., 10,
15   3979–4003, https://doi.org/10.5194/gmd-10-3979-2017, 2017.

Overpeck, J., Otto-Bliesner, B. L., Miller, G., Muhs, D., Alley, R., and Kiehl, J.: Paleoclimatic Evidence for Future Ice-Sheet Instability and Rapid Sea-Level Rise, Science, 311, 1747–1750, https://doi.org/10.1126/science.1115159, 2006.

Paterson, W.: The Physics of Glaciers (3rd edn), Pergamon Press, Oxford, 1994.

Pattyn, F.: A new three-dimensional higher-order thermomechanical ice sheet model: Basic sensitivity, ice stream development, and ice flow
20   across subglacial lakes, Journal of Geophysical Research: Solid Earth, 108, https://doi.org/10.1029/2002JB002329, 2003.

Pfeffer, W. T., Harper, J. T., and O'Neel, S.: Kinematic Constraints on Glacier Contributions to 21st-Century Sea-Level Rise, Science, 321, 1340–1343, https://doi.org/10.1126/science.1159099, 2008.

Plach, A., Nisancioglu, K. H., Le clec'h, S., Born, A., Langebroek, P. M., Guo, C., Imhof, M., and Stocker, T. F.: Eemian Greenland Surface Mass Balance strongly sensitive to SMB model choice, Clim. Past Discussions, pp. 1–37, https://doi.org/10.5194/cp-2018-81, 2018.

25 Pollard, D. and DeConto, R. M.: Modelling West Antarctic ice sheet growth and collapse through the past five million years, Nature, 458, 329–332, https://doi.org/10.1038/nature07809, 2009.

Pollard, D. and DeConto, R. M.: Description of a hybrid ice sheet-shelf model, and application to Antarctica, Geosci. Model Dev., 5, 1273–1295, https://doi.org/10.5194/gmd-5-1273-2012, 2012.

Price, S. F., Payne, A. J., Howat, I. M., and Smith, B. E.: Committed sea-level rise for the next century from Greenland ice sheet dynamics
30   during the past decade, Proceedings of the National Academy of Sciences, 108, 8978–8983, https://doi.org/10.1073/pnas.1017313108, 2011.

Quiquet, A., Ritz, C., Punge, H. J., and Salas y Mélia, D.: Greenland ice sheet contribution to sea level rise during the last interglacial period: a modelling study driven and constrained by ice core data, Clim. Past, 9, 353–366, https://doi.org/10.5194/cp-9-353-2013, 2013.

Raynaud, D., Chappellaz, J., Ritz, C., and Martinerie, P.: Air content along the Greenland Ice Core Project core: A record of surface climatic
35   parameters and elevation in central Greenland, Journal of Geophysical Research: Oceans, 102, 26 607–26 613, https://doi.org/10.1029/97JC01908, 1997.

Rignot, E. and Mouginot, J.: Ice flow in Greenland for the International Polar Year 2008–2009, Geophysical Research Letters, 39, L11 501, https://doi.org/10.1029/2012GL051634, 2012.

Robel, A. A. and Tziperman, E.: The role of ice stream dynamics in deglaciation, Journal of Geophysical Research: Earth Surface, 121, 2016JF003 937, https://doi.org/10.1002/2016JF003937, 2016.

Robinson, A., Calov, R., and Ganopolski, A.: Greenland ice sheet model parameters constrained using simulations of the Eemian Interglacial, Clim. Past, 7, 381–396, https://doi.org/10.5194/cp-7-381-2011, 2011.

5 Schlegel, N.-J., Larour, E., Seroussi, H., Morlighem, M., and Box, J. E.: Decadal-scale sensitivity of Northeast Greenland ice flow to errors in surface mass balance using ISSM, Journal of Geophysical Research: Earth Surface, 118, 667–680, https://doi.org/10.1002/jgrf.20062, 2013.

Shapiro, N. and Ritzwoller, M.: Inferring surface heat flux distributions guided by a global seismic model: particular application to Antarctica, Earth and Planetary Science Letters, 223, 213–224, https://doi.org/10.1016/j.epsl.2004.04.011, 2004.

10 Stone, E. J., Lunt, D. J., Annan, J. D., and Hargreaves, J. C.: Quantification of the Greenland ice sheet contribution to Last Interglacial sea level rise, Clim. Past, 9, 621–639, https://doi.org/10.5194/cp-9-621-2013, 2013.

Straneo, F. and Heimbach, P.: North Atlantic warming and the retreat of Greenland's outlet glaciers, Nature, 504, 36–43, doi:10.1038/nature12854, http://www.nature.com/nature/journal/v504/n7478/abs/nature12854.html, 2013.

Tabone, I., Blasco, J., Robinson, A., Alvarez-Solas, J., and Montoya, M.: The sensitivity of the Greenland Ice Sheet to glacial–interglacial
15 oceanic forcing, Clim. Past, 14, 455–472, https://doi.org/10.5194/cp-14-455-2018, 2018.

Yin, Q. and Berger, A.: Interglacial analogues of the Holocene and its natural near future, Quaternary Science Reviews, 120, 28–46, https://doi.org/10.1016/j.quascirev.2015.04.008, 2015.

Zwally, H. J., Abdalati, W., Herring, T., Larson, K., Saba, J., and Steffen, K.: Surface Melt-Induced Acceleration of Greenland Ice-Sheet Flow, Science, 297, 218–222, https://doi.org/10.1126/science.1072708, 2002.